Study of the catalytic species metallocene/MAO and metallocene/TMA by cyclic voltammetry

Fábio G. Costa, Lílian M.T. Simplício, Zênis N. da Rocha, Soraia T. Brandão*

Instituto de Química da Universidade Federal da Bahia, Campus de Ondina, Salvador 40170-290, Brazil

Abstract

In this paper, an electrochemical study of the metallocene/methylaluminoxane (MAO) and metallocene/trimethylaluminium (TMA) species is presented. The metallocenes used were $[(CH_3)_2Si(Cp)_2ZrCl_2]$ and $[(Cp)_2ZrCl_2]$. The evaluation of the Metallocene/MAO and Metallocene/TMA systems was based on the analysis of the redox potentials of the solutions with different Al/Zr molar ratios using acetonitrile as solvent. The results obtained for Al/Zr ratios lower than 30, suggested that in presence of TMA or MAO, the formed monomethylated species are $[(L)Zr^{IV}(CH_3)Cl]$, L = cyclopentadienyl $(Cp)_2$ or $(CH_3)_2Si(Cp)_2$. For Al/Zr molar ratios higher than 30, the results obtained in TMA presence are in agreement with the formation of the species $[(L)Zr^{IV}(CH_3)(\mu\text{-}CH_3)Al(CH_3)_2]^+$, while in MAO presence the ionic pair, $[(L)Zr^{IV}CH_3]^+[MAOCl]^-$, is formed. There's a general agreement that these are active species in olefin polymerization.
© 2003 Elsevier B.V. All rights reserved.

Keywords: Zirconocenes; Polymerization; Ethylene; Cyclic voltammetry

1. Introduction

Metallocene catalysts in the presence of an alkylaluminum cocatalyst are very efficient in α-olefin polymerization offering a great versatility in the synthesis and control of the structure of polyolefins compared with conventional Ziegler–Natta catalysts. Metallocene/methylaluminoxane (MAO) systems combine high activity with the possibility of tailoring polymer properties such as molecular weight and molecular weight distribution as well as stereochemical structure [1–8].

Due to the important role of MAO and trimethylaluminium (TMA) as cocatalyst in α-olefin polymerization using metallocene, the characterization of the catalytic active species and the elucidation of the mechanism involved in the activation of the metallocene by the cocatalyst have been a target of several studies reported in [9–13].

Studies in [14–18] proposed that the reaction with metallocene and MAO leads the formation of $[L_2MtX]^+[MAOCl]^-$ species in which Mt = Ti, Zr, Hf; X = Cl, CH_3, and L = cyclopentadienyl (Cp), indenyl (Ind), fluorenyl (Fluo).

There's a general agreement that this is the active species in olefin polymerization.

Spectroscopic studies in the region of ultraviolet–visible and electric conductivity measurements carried out on the system *rac*-[Et(Ind)$_2$ZrCl$_2$]/MAO, using several Al/Zr molar ratios [19,20] had considered that for Al/Zr molar ratios lower than 30 the metallocene and MAO reaction occurs with a monomethylation of the metallocene by "free" TMA present in the MAO solution. For Al/Zr molar ratios higher than 30 this reaction provides the formation of the ionic pair between cation metallocene and anion MAO.

Recently, Cramail and coworkers [21–23] investigated the distinct roles of MAO and TMA in the metallocene activation process and showed that the use of "TMA-depleted" MAO (MAO solution containing a very low concentration of TMA) offers the possibility to activate zirconocene at rather low Al/Zr ratios in homogeneous conditions (Al/Zr 50–200), proposing that the presence of TMA leads to the formation of a species, less active in olefin polymerization, underlining the poisoning role of TMA in MAO in the metallocene activation process.

In this context the present paper describes a study of the catalytic species Metallocene/MAO and metallocene/TMA by cyclic voltammetry based on the cathodic peaks shift of the solutions containing different Al/Zr molar ratios in order

* Corresponding author. Tel.: +55-712-375-784;
fax: +55-712-374-117.
E-mail address: brandao@ufba.br (S.T. Brandão).

to understand the mechanism involved in the activation of zirconocene by the cocatalyst and the nature of the active species in olefin polymerization.

2. Experimental part

2.1. Chemicals

All experimental procedures had been carried under inert atmosphere using Schlenk techniques. Acetonitrile (Merck, spectroscopic grade) used as solvent in the cyclic voltammetry experiments was dried in molecular sieve. Tetrabutilammonium tetrafluorborate (Merck), was used without further purification. MAO (15% in toluene) and TMA (12% in toluene) had been supplied by Akzo Nobel and the metallocenes, $[(Cp)_2ZrCl_2]$ and $[(CH_3)_2SiCp_2ZrCl_2]$ had been supplied by Strem.

2.2. Electrochemical measurements

The cyclic voltammograms were taken with a potentiostat/galvanostat, PARC, model 273. All experiments were carried out using a conventional three-electrode cell. Glassy carbon was used as working electrode. An Ag/AgCl electrode was used as the reference electrode and a platinum wire as the auxiliary electrode. Electrochemical data were obtained using $0.1\,mol\,l^{-1}$ solutions of tetrabutilammonium and tetrafluoroborate in acetonitrile as supporting electrolyte. In the cyclic voltammograms, neither anodic nor cathodic peaks were observed in the absence of metallocene in the potential range studied. All solutions were deaerated by bubbling high purity argon. The cocatalyst solutions were prepared with different Al/Zr molar ratios between 0 and 50 and the cyclic voltammograms were recorded with scan rate of $100\,mV\,s^{-1}$.

2.3. Polymerization reactions

The reaction was carried in a 300 ml Parr reactor previously dried and inertized with nitrogen. The Schlenk technique was used to prevent reagents contact with air. The reagents were added to the reactor in the following sequence: toluene solution, MAO solution, metallocene catalyst and ethylene. The reaction lasted for 1 h under mechanical agitation of 650 rpm, temperature of 70 °C and ethylene pressure of 15 psi in the reactor. After the reaction the polymers had been filtered on vacuum, washed with ethanol excess and dried at 40 °C.

3. Results and discussion

Cyclic voltammograms of the metallocenes investigated are illustrated in Fig. 1. The current-potential profiles are very similar for both of them. When the potential scan
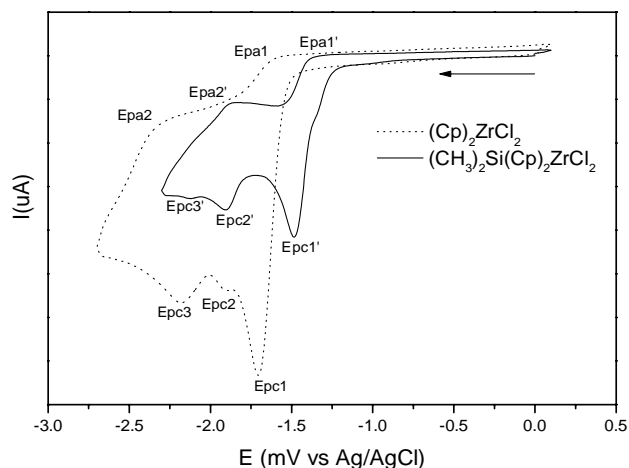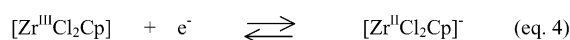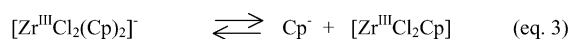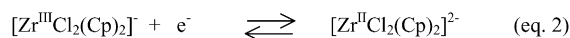

Fig. 1. Cyclic voltammograms of the metallocenes $[(Cp)_2ZrCl_2]$ and $[(CH_3)_2Si(Cp)_2ZrCl_2]$.

begins at 0.0 V and goes toward negative potentials, three well defined cathodic peaks can be observed. The cyclic voltammogram of $[(Cp)_2ZrCl_2]$ depicts these three peaks at $-1.7\,V$ (Epc1), $-1.9\,V$ (Epc2) and $-2.2\,V$ (Epc3) and anodic peaks at $-1.65V$ (Epa1) and $-2.3\,V$ (Epa2) corresponding to the first and last cathodic peaks. The complex $[(CH_3)_2Si(Cp)_2ZrCl_2]$ depicts these peaks at $-1.48\,V$ (Epc1′), $-1.91\,V$ (Epc2′) and $-2.12\,V$ (Epc3′) and anodic peaks at $-1.42\,V$ (Epa1′) and $-1.86\,V$ (Epa2′) corresponding to the first and the second cathodic peaks. All potentials were reported versus Ag/AgCl.

The cathodic peak with a less negative potential value is attributed to the electrode process in which the $[(Cp)_2Zr^{IV}Cl_2]$ complex is reduced and leads to the formation of $[(Cp)_2Zr^{III}Cl_2]^-$ species (Eq. (1) in Scheme 1). This Zr(III) species can be reduced with the process involving one electron forming $[(Cp)_2Zr^{II}Cl_2]^{2-}$ and justifying the cathodic peak at $-1.9\,V$ (Eq. (2) in Scheme 1). Studies in [24] have evidenced the possibility of a Cp^- ring loss in the $[(Cp)_2Zr^{III}Cl_2]$ species, then the cathodic peak at $-2.2\,V$ can be assigned to the Zr^{III}/Zr^{II} redox process in the $[(Cp)Zr^{III}Cl_2]^-$ species (Eqs. (3) and (4) in Scheme 1).

The cathodic peaks observed for the $[(CH_3)_2Si(Cp)_2 Zr^{IV}Cl_2]$ complex are assigned to the analogous electrode processes described for the $[(Cp)_2Zr^{IV}Cl_2]$ complex. The proposal for the $[(CH_3)_2Si(Cp)_2Zr^{III}Cl_2]^-$ species and its

$$[Zr^{IV}Cl_2(Cp)_2] \;+\; e^- \;\rightleftharpoons\; [Zr^{III}Cl_2(Cp)_2]^- \qquad (eq.\ 1)$$

$$[Zr^{III}Cl_2(Cp)_2]^- \;+\; e^- \;\rightleftharpoons\; [Zr^{II}Cl_2(Cp)_2]^{2-} \qquad (eq.\ 2)$$

$$[Zr^{III}Cl_2(Cp)_2]^- \;\rightleftharpoons\; Cp^- \;+\; [Zr^{III}Cl_2Cp] \qquad (eq.\ 3)$$

$$[Zr^{III}Cl_2Cp] \;+\; e^- \;\rightleftharpoons\; [Zr^{II}Cl_2Cp]^- \qquad (eq.\ 4)$$
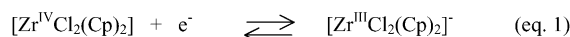
Scheme 1. Global electrode process reactions for $[(Cp)_2ZrCl_2]$.
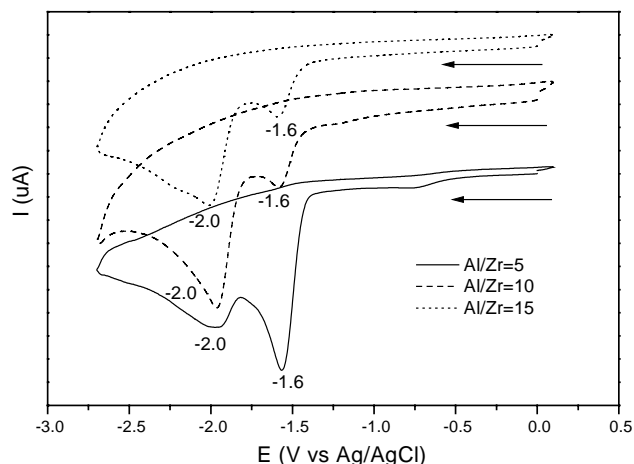
Fig. 2. Cyclic voltammograms of the [Cp$_2$ZrCl$_2$] in the presence of MAO, Al/Zr < 30.

Fig. 3. Cyclic voltammograms of [Cp$_2$ZrCl$_2$] in the presence of MAO (Al/Zr = 30).
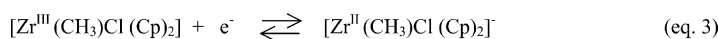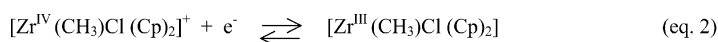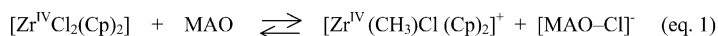
consequent reduction is an analogy to the [(Cp)$_2$Zr^{III}Cl$_2$]$^-$ complex. The obtained results indicated that there is no other one-third peak so defined as in the [(Cp)$_2$ZrCl$_2$] species. For the [(CH$_3$)$_2$Si(Cp)$_2$Zr^{III}Cl$_2$]$^-$ complex only a barely discernible shoulder appears at −2.12 V.

This discernible shoulder indicates that the reaction of a Cp$^-$ ring loss in this complex is slower than in the [(Cp)$_2$Zr^{III}Cl$_2$]$^-$ species. This can be explained by the fact that the existence of a (CH$_3$)$_2$Si in the [(CH$_3$)$_2$Si(Cp)$_2$Zr^{III}Cl$_2$]$^-$ complex probably inertizes the cyclopentadienyl, thus, this reaction becomes slower than the analogue reaction in [(Cp)$_2$Zr^{III}Cl$_2$]$^-$ complex.

3.1. Cyclic voltammogram of [(Cp)$_2$ZrCl$_2$] in presence of MAO

The cyclic voltammograms of the solutions containing Al/Zr ratios of 5, 10 and 15 are shown in Fig. 2. The run of potential begins at 0.0 V and goes toward negative potential, where two cathodic peaks at −1.6 and −2.0 V are observed.

UV/visible spectroscopy studies [19,20] indicated that the addition of small amounts of MAO (0 < Al/Zr < 15) to rac-[Et(Ind)$_2$ZrCl$_2$] leads to the substitution of one chloride atom by a methyl group. Thus, in analogy with this proposal, Scheme 2 shows the reactions involved in the electrochemical process for the monomethylated species. In a first step the [(Cp)$_2$Zr^{IV}(CH$_3$)Cl]$^+$ complex is formed, followed by reduction in the electrode surface at −1.6 V forming

[(Cp)$_2$Zr^{III}(CH$_3$)Cl] (Eq. (2) in Scheme 2). In addition there is another electrode process, since the formed Zr(III) species can be reduced to [(Cp)$_2$Zr^{II}(CH$_3$)Cl]$^-$ at −2.0 V.

On the other hand, the addition of incremental amounts of MAO solution (Al/Zr = 30) results in a cyclic voltammogram with only one cathodic peak at −2.6 V (Fig. 3). This value is more negative than the others obtained for the electrode process in [(Cp)$_2$Zr^{IV}(Cl)$_2$] for Al/Zr molar ratios lower than 30. This result indicates the formation of a species in which the IV oxidation state is more stable.

This peak at −2.6 V can be attributed to the reduction process involving one electron in [(Cp)$_2$Zr^{IV}CH$_3$]$^+$[MAOCl]$^-$ considered as an active species in olefin polymerization [14–18]. An hypothetical structure for the highly active species for olefin polymerization indicated the presence of a cation–methylzirconocene and a MAO–Cl counter anion (Structure I). Similar species were reported by spectroscopic studies when "TMA-depleted" MAO (Al/Zr ≈ 150) was added to rac-[Et(Ind)$_2$ZrCl$_2$] [23]. In this case a reverse bathochromic shift of the zirconocene main absorption band from 396 to 440 nm was observed. This shift was attributed to an important decrease of the zirconium electronic density [23]. Considering this behavior, a shift to less negative potential in the cyclic voltammograms should be expected. However, this behavior is not observed, probably due to the interaction between cation–methylzirconocene and MAO-Cl, which stabilizes Zr(IV) in this structure.

[Zr^{IV}Cl$_2$(Cp)$_2$] + MAO $\rightleftarrows$ [Zr^{IV}(CH$_3$)Cl (Cp)$_2$]$^+$ + [MAO–Cl]$^-$ (eq. 1)

[Zr^{IV}(CH$_3$)Cl (Cp)$_2$]$^+$ + e$^-$ $\rightleftarrows$ [Zr^{III}(CH$_3$)Cl (Cp)$_2$]   (eq. 2)

[Zr^{III}(CH$_3$)Cl (Cp)$_2$] + e$^-$ $\rightleftarrows$ [Zr^{II}(CH$_3$)Cl (Cp)$_2$]$^-$ (eq. 3)

Scheme 2. Global electrode process reactions for [Cp$_2$ZrCl$_2$]/MAO, Al/Zr < 30.

Structure (I)-Hypothetical structure of catalytic active species of polymerization
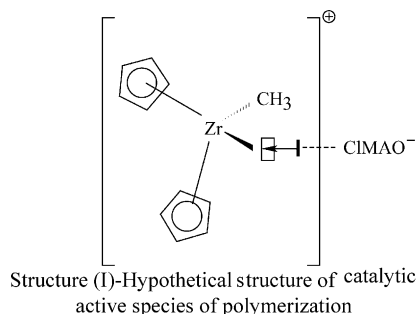
These studies [23] proposed that the species showed in Structure I can be either inactive when formed with commercial MAO or active, when they result from the use of "TMA-depleted" MAO. The deactivation of this species is attributed to the presence in commercial MAO of TMA remaining from its partial hydrolysis.

3.2. Cyclic voltammograms of zirconocene in presence of TMA

The cyclic voltammograms obtained for $[(Cp)_2ZrCl_2]$ and $[(CH_3)_2Si(Cp)_2ZrCl_2]$ in presence of TMA for different Al/Zr molar ratios are illustrated in Figs. 4 and 5, respectively. For Al/Zr molar ratios lower than 30, when the run of potential begins at 0.0 V and goes towards negative potential, two cathodic peaks can be observed. For $[(Cp)_2ZrCl_2]$ the potentials are -1.6 and -1.9 V; for $[(CH_3)_2Si(Cp)_2ZrCl_2]$ the potentials are -1.5 V and -1.9 V and anodic peak at -1.4 V corresponding to the first cathodic peak. The same shift for the cathodic peaks was related for $[(Cp)_2ZrCl_2]$ in MAO presence for these Al/Zr molar ratios.

These results suggest that the two cathodic peaks are assigned as $Zr^{IV/III}$ and $Zr^{III/II}$ reduction in monomethylated species as described in Scheme 2. Thus, in the presence of MAO or TMA cocatalyst, with Al/Zr molar ratios lower than 30, the electrode process indicated the presence of the
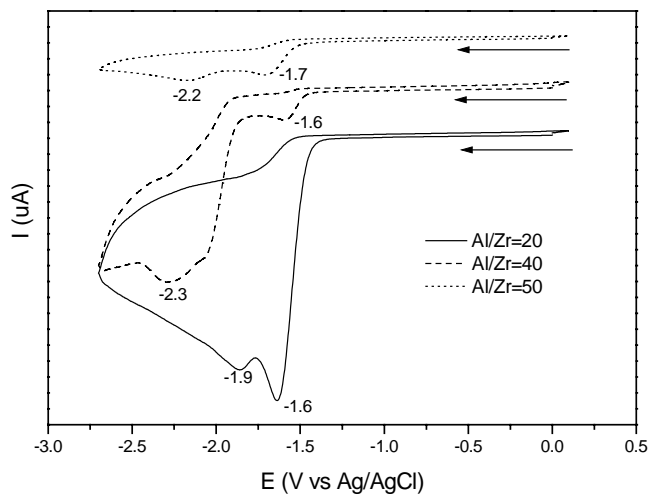

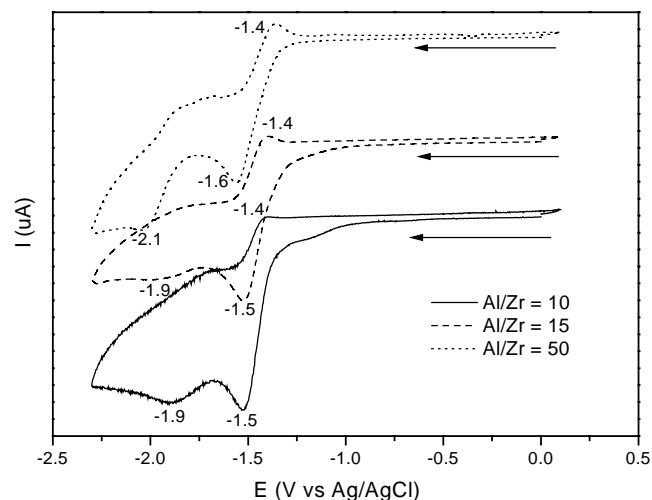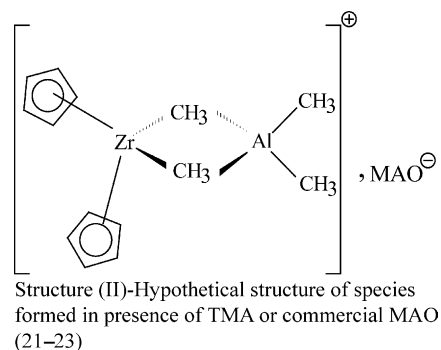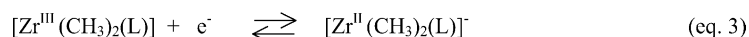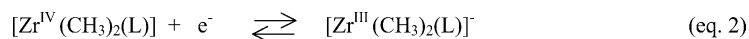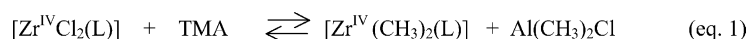Fig. 5. Cyclic voltammograms of $[(CH_3)_2Si(Cp)_2ZrCl_2]$ in presence of TMA.

same zirconocene species. These results are in agreement with [19,20].

For Al/Zr molar ratios higher than 30, two well defined cathodic peaks are also observed. However these peaks are shifted to more negative potentials when compared to the corresponding peaks for Al/Zr ratios lower than 30. This result indicates that besides the formation of a monomethylated species, one another with a more difficult reduction process is also formed. In agreement with [19,20], Al/Zr ratios higher than 30 in TMA presence would lead the formation of dimethylated species, $[(L)Zr^{IV}(CH_3)(\mu\text{-}CH_3)Al(CH_3)_2]^+$, L = $(Cp)_2$, $(CH_3)_2Si(Cp)_2$, showed in Structure II. Thus, the two observed peaks are assigned as $Zr^{IV/III}$ and $Zr^{III/II}$ reduction in these species. Scheme 3 shows the reactions involved in the electrode process. The cyclic voltammograms obtained for the complex $[(CH_3)_2Si(Cp)_2ZrCl_2]/TMA$ shows, besides the cathodic peak, an anodic corresponding to the first cathodic peak.

Fig. 4. Cyclic voltammograms of $[Cp_2ZrCl_2]$ in the presence of TMA.

Structure (II)-Hypothetical structure of species formed in presence of TMA or commercial MAO (21–23)

Studies in [22,23] have proposed that large amounts of TMA present in MAO solution leads to the formation of a complexed structure between TMA and cationic zirconocene. This species shows similar catalytic activity in olefin polymerization when compared with that one formed

$$[Zr^{IV}Cl_2(L)] \; + \; TMA \quad \rightleftarrows \quad [Zr^{IV}(CH_3)_2(L)] \; + \; Al(CH_3)_2Cl \qquad (eq.\ 1)$$

$$[Zr^{IV}(CH_3)_2(L)] \; + \; e^- \quad \rightleftarrows \quad [Zr^{III}(CH_3)_2(L)]^- \qquad (eq.\ 2)$$

$$[Zr^{III}(CH_3)_2(L)] \; + \; e^- \quad \rightleftarrows \quad [Zr^{II}(CH_3)_2(L)]^- \qquad (eq.\ 3)$$

Scheme 3. Global electrode process reactions in zirconocene TMA Al/Zr > 30.

in MAO presence and showed in Structure I [22]. These results are in agreement with the electrode potential for these species, whose values are similar, indicating the formation of species with similar stabilities.

As can be seen the cathodic peak attributed to the $Zr^{IV/III}$ reduction process for $[(Cp)_2ZrCl_2]$ or $[(CH_3)_2Si(Cp)_2ZrCl_2]$, in MAO or TMA presence, is shifted for a lower potential than in absence of the cocatalyst. However these results are not expected, since the substitution of one chloride atom by one methyl group from the cocatalysts, MAO or TMA, increases the electronic density in the zirconium(IV) and would lead the reduction process to occur in a more negative potential.

One explanation for these results should be that with the addition of MAO or TMA solutions, which solvent is toluene, there is a change in the polarity of the solutions. As can be seen, the effect of chloride σ donor electron properties is clear when compared to methyl at Al/Zr molar ratios higher than 30.

The eletrochemical results shows that the supposed active species in olefin are formed at low Al/Zr ratios (Al/Zr ≈ 50), indeed there's a general agreement that the addition of larger amounts commercial MAO (Al/Zr ratio > 1000) is necessary to prevent the catalyst deactivation [1–7].

3.3. Correlation with catalytic deactivation for ethylene polymerization with potential reduction of zirconocenes

The Cyclic voltammograms of the metallocenes investigated (Fig. 1) shows that the cathodic peak attributed to the $Zr^{IV/III}$ redox process for $[(CH_3)_2Si(Cp)_2ZrCl_2]$ is at −1.48 V and for $[(Cp)_2ZrCl_2]$ at −1.7 V, indicating that the $Zr^{IV/III}$ reduction process is less difficult in the $[(CH_3)_2Si(Cp)_2ZrCl_2]$ complex. This difference can be explained by the fact that in this complex, the $(CH_3)_2Si$ bridge decreases the electronic density in the zirconium and leads this metallic center a stronger Lewis acid than the same metallic ion in the $[(Cp)_2ZrCl_2]$ complex. This decrease in the electronic density is a consequence of the π-acceptor properties of the silicon.

As can be seen in Table 1 and in Fig. 6 the catalytic activity is higher for $[(CH_3)_2Si(Cp)_2ZrCl_2]$ than $[(Cp)_2ZrCl_2]$. On the basis of the active species nature in α-olefin polymerization and the important role of the IV oxidation state, the activity should be higher for $[(Cp)_2ZrCl_2]$, since the IV oxidation state in this complex

Table 1
Deactivation tests of the catalysts in ethylene polymerization

Time (min)	$[(Cp)_2ZrCl_2]$[a]	$[(CH_3)_2Si(Cp)_2ZrCl_2]$[a]
15	317.04	360.98
30	169.88	169.19
45	97.46	113.17
60	88.36	82.67

[a] Activity: $KgPE\,molZr^{-1}\,h^{-1}\,atm^{-1}$.

is more stable. However, in order to analyze this activity, it is important to consider the zirconocene–olefin interaction. Considering that in $[(CH_3)_2Si(Cp)_2ZrCl_2]$ complex, the zirconium is more acidic than in $[(Cp)_2ZrCl_2]$, the cation–methylzirconocene/MAOCl interaction with ethylene would be favored, justifying the higher activity observed for the $[(CH_3)_2Si(Cp)_2ZrCl_2]$ complex. According to [25], the activity of these systems are also affected by steric effects. Thus, the higher activity observed for this complex is a result of electric and steric effects.

According to the results showed in Table 1 and Fig. 6, in the initial stages the catalytic activity decreasing is higher for $[(CH_3)_2Si(Cp)_2ZrCl_2]$. This results suggest that the potential redox has a primary effect when compared to zirconocene–olefin interaction, since the $Zr^{IV/III}$ reduction process is less difficult in the $[(CH_3)_2Si(Cp)_2ZrCl_2]$ complex. After a few minutes the plateau of minimum activity is reached.
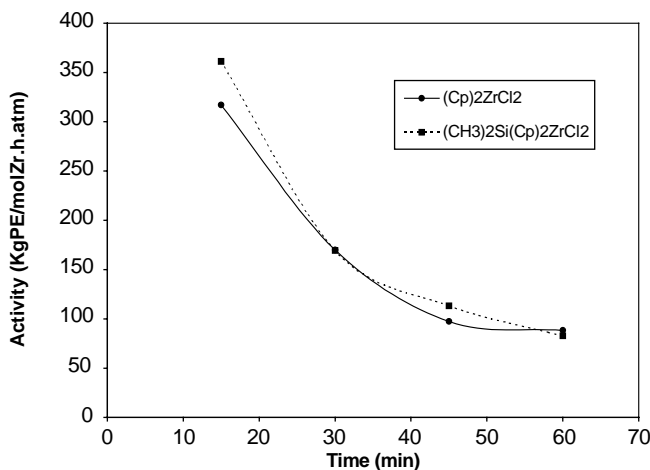

Fig. 6. Activity versus time curves obtained for $[(Cp)_2ZrCl_2]$ and $[(CH_3)_2Si(Cp)_2ZrCl_2]$.

4. Conclusions

The results obtained with the cyclic voltammetry comparative study for $[(Cp)_2ZrCl_2]$ and $[(CH_3)_2Si(Cp)_2ZrCl_2]$ systems suggest that for Al/Zr molar ratios lower than 30, in TMA or MAO presence, the formed monomethylated species are the same. In the systems containing MAO, the formation of this species are favored by the "free" TMA in solution.

For Al/Zr molar ratios higher than 30 the results suggest that in MAO presence the ionic pair $[(L)Zr^{IV}Cl]^+[MAOCl]^-$ is formed, while TMA presence leads to the formation of a dimethylated specie, $[(L)Zr^{IV}(CH_3)(\mu\text{-}CH_3)Al(CH_3)_2]^+$. According to the literature data, this species have similar activity in olefin polymerization.

The eletrochemical results shows that these species are formed with low Al/Zr ratios (Al/Zr $\approx$ 50), indeed there's a general agreement that the addition of larger amounts commercial MAO (Al/Zr ratio > 1000) is necessary to prevent the catalyst deactivation.

Acknowledgements

References

[1] H.G. Alt, A. Köppl, Chem. Rev. 100 (2000) 1205.
[2] H.-H. Brintzinger, D. Fischer, R. Mülhaupt, B. Rieger, R. Waymouth, Angew Chem. 107 (1995) 1255; H.-H. Brintzinger, D. Fischer, R. Mülhaupt, B. Rieger, R. Waymouth, Angew. Chem. Int. Ed. Engl. 34 (1995) 1143.
[3] W. Kaminsky, Catal. Today 62 (2000) 23.
[4] W. Kaminsky, R. Steiger, Polyhedron 7 (1988) 2375.
[5] W. Kaminsky, A. Laban, Appl. Catal. 222 (2001) 47.
[6] C. Götz, A. Rau, G. Luft, J. Mol. Catal. 184 (2002) 95.
[7] J.C.W. Chien, D. He, J. Pol. Sci. 29 (1991) 1603.
[8] W. Kaminsky, J. Chem. Soc. Dalton Trans. (1998) 1413.
[9] F. Ciardelli, A. Altomare, M. Michelotti, Catal. Today. 41 (1998) 149.
[10] J.C.W. Chien, W. Tsai, M.D. Rausch, J. Am. Chem. Soc. 113 (1991) 8570.
[11] J.C.W. Chien, W. Song, M.D. Rausch, Macromolecules 26 (1993) 3239.
[12] W. Kaminsky, Macromol. Symp. 97 (1995) 79.
[13] W. Kaminsky, C. Sttrübel, J. Mol. Catal. 128 (1998) 191.
[14] C. Sishta, R.M. Hathorn, T.J. Marks, J. Am. Chem. Soc. 114 (1992) 1112.
[15] I. Tritto, S. Li, M.C. Sacchi, G. Zannoni, Macromolecules 26 (1993) 7111.
[16] M. Bochman, J. Chem. Soc. Dalton Trans. (1996) 225.
[17] I. Tritto, R. Donetti, M.C. Sacchi, P. Locatelli, G. Zannoni, Macromolecules 30 (1997) 1247.
[18] I. Tritto, R. Donetti, M.C. Sacchi, P. Locatelli, G. Zannoni, Macromolecules 32 (1999) 264.
[19] D. Coevoet, H. Cramail, A. Deffieux, Macromol. Chem. Phys. 199 (1998) 1451.
[20] D. Coevoet, H. Cramail, A. Deffieux, Macromol. Chem. Phys. 199 (1998) 1459.
[21] J. Pédeutour, H. Cramail, A. Deffieux, J. Mol. Catal. 176 (2001) 87.
[22] J. Pédeutour, H. Cramail, A. Deffieux, J. Mol. Catal. 174 (2001) 81.
[23] J. Pédeutour, K. Radhakrishnan, H. Cramail, A. Deffieux, J. Mol. Catal. 185 (2002) 119.
[24] N. El Murr, A. Chaloyard, J. Tirouflet, J. Chem. Soc. (1980) 446.
[25] J.A. Ewen, M.J. Elder, C.J. Harlan, L. Jones, Polymer Preprints 1 (1991) 496.